Turbulent kinetic energy generated by wind farms is treated incorrectly in the WRF model

Cristina L. Archer*

Sicheng Wu

Yulong Ma

Center for Research in Wind (CReW), University of Delaware, Newark, Delaware, USA

Pedro A. Jiménez

National Center for Atmospheric Research (NCAR), Boulder, Colorado, USA

**Corresponding author address:* Integrated Science and Engineering Laboratory (ISELab), University of Delaware, 221 Academy St, Newark, DE 19716, USA

E-mail: carcher@udel.edu

ABSTRACT

As wind farms grow in number and size worldwide, it is important that their potential impacts on the environment are studied and understood. The Fitch parameterization implemented in the Weather Research and Forecasting (WRF) model since version 3.3 is a widely used tool today to study such impacts. We identified two important issues related to the way the added turbulent kinetic energy (TKE) generated by a wind farm is treated in the WRF model with the Fitch parameterization. The first issue is a simple bug in the WRF code and the second issue is the excessive value of a coefficient that relates TKE to the turbine electro-mechanical losses, called C_{TKE}. These two issues directly affect the way a wind farm wake evolves and they impact properties like near-surface temperature and wind speed at the wind farm as well as behind it in the wake. We provide a bug fix and a revised value of C_{TKE} that is one quarter of the original value. We present the results obtained with the Fitch parameterization in the WRF model for a single turbine with and without the bug fix and the corrected C_{TKE} and compare them against high-fidelity Large-Eddy Simulations (LES). These two issues have not been discovered before because they interact with one another in such a way that their combined effect is a somewhat realistic vertical TKE profile at the wind farm and a realistic wind speed deficit in the wake. All WRF simulations that used the Fitch wind farm parameterization are affected and their conclusions may need to be revisited.

1. Introduction

The issue of potential impacts of wind farms was first introduced in 2004 by two seminal papers: Keith et al. (2004) at the global scale using a climate model and Baidya Roy et al. (2004) at the regional scale using a mesoscale model. Since the resolution of both models was not fine enough to resolve the flow around the turbines, a wind farm parameterization was needed, which is a way to introduce sub-grid scale effects into the resolved grid.

Keith et al. (2004) used a very simple parameterization: they treated wind farms as added surface roughness. A few other studies later used the same idea and approximated turbines as either increased surface roughness or increased surface drag elements (Kirk-Davidoff and Keith 2008; Barrie and Kirk-Davidoff 2010; Wang and Prinn 2010; Miller et al. 2011). These simple parameterizations have all been dismissed, because wind turbines do not extract energy near the surface but rather around hub height, i.e., 80 -– 120 m (Jacobson and Archer 2012; Fitch et al. 2013).

The wind farm parameterization by Baidya Roy et al. (2004) was more advanced because it treated wind turbines as elevated (i.e., above the surface) sinks of momentum and sources of turbulent kinetic energy (TKE). As reviewed in Pan and Archer (2018), many studies have been published since with the same principle of representing wind turbines as elevated momentum sinks, although with various different approaches with respect to power generation and added TKE (Blahak et al. 2010; Jacobson and Archer 2012; Marvel et al. 2013; Adams and Keith 2013; Abkar and Porté-Agel 2015a; Volker et al. 2015; Vollmer et al. 2016; Pan and Archer 2018). The Fitch parameterization (Fitch et al. 2012) was among them. Because it was incorporated directly in the Weather Research and Forecasting (WRF) model in April 2011 in version 3.3 and because the WRF model is the most widely used mesoscale model, the Fitch parameterization quickly became the most commonly used tool to study regional to large-scale impacts of wind farms. However, as described in Sections 3b-c, a code bug and the excessive value of a coefficient seriously affect any results obtained with the Fitch parameterization.

A complete literature review of past studies that have used the Fitch parameterization within the WRF model and therefore were affected by the two issues is not possible, as the relevant WRF settings were not always disclosed. We just report that at least 20 papers were published since 2011 that used the Fitch parameterization within WRF v3.3 or later and their conclusions are therefore impacted by the two issues discussed below, although we do not know to which extent.

2. The two issues and their solutions

a. The Fitch parameterization

The coded version of the Fitch parameterization in WRF has gone through development and modifications by the scientific community throughout the years and therefore it is no longer the same as in the original formulation by Fitch et al. (2012). Here we focus on the latest version (WRF v4.1).

The first step of the Fitch parameterization is the calculation of the power generated by the turbines in each grid cell. Since the power curve, provided in input file `wind-turbine.tbl`, is a function of hub-height wind speed, interpolation of horizontal wind speed from the vertical levels that surround the hub height is performed and then the power generated by the turbine (P) is obtained from the power curve. If multiple turbines are present in the same grid cell, regardless of their actual position, the total power at the grid cell is calculated as the sum of the power generated by each turbine, thus wake losses within the grid cell are neglected. This problem was discussed at length in Pan and Archer (2018) and it causes, in general, an overestimation of the power generated in grid cells with multiple turbines. Since this problem could obscure or complicate the effect of the two issues that are the object of this study, only single-turbine simulations will be conducted in Section 3a.

After calculating the power P from the modelled hub-height wind speed U_h and the manufacturer power curve, the power coefficient C_P is estimated via this equation:

$$P = \frac{1}{2} A \rho C_P U_h^3, \tag{1}$$

where ρ is the air density (set to a constant, 1.23 kg m^{-3}) and A is the turbine rotor area. Once C_P is known, the coefficient C_{TKE}, defined as:

$$C_{TKE} = C_T - C_P, \tag{2}$$

where the thrust coefficient C_T is given in input file `wind-turbine.tbl` as a function of U_h, can be calculated and used later to determine TKE (Eq. 3). More details about C_P and C_T are given in Section 2c.

To obtain the vertical distribution of TKE and velocity, the basic principle is that each vertical level k that intersects the rotor contributes proportionally to the fractional rotor area contained in that level (A_k) and to the horizontal wind speed at that level (U_k):

$$\frac{\partial TKE_k}{\partial t} = \frac{1}{2} \frac{A_k C_{TKE} U_k^3}{(z_{k+1} - z_k)}, \tag{3}$$

$$\frac{\partial u_k}{\partial t} = -\frac{1}{2} \frac{A_k C_T U_k u_k}{(z_{k+1} - z_k)}, \tag{4}$$

$$\frac{\partial v_k}{\partial t} = -\frac{1}{2} \frac{A_k C_T U_k v_k}{(z_{k+1} - z_k)}, \tag{5}$$

where u_k and v_k are the horizontal wind components and z_k is the height of vertical level k. Eq. 3 to 5 are multiplied by a correction factor if energy conservation is not met across the rotor. If multiple turbines are present in the same grid cell, each will add the exact same contribution to the TKE and momentum tendencies as in Eq. 3 through 5.

In the WRF code, the Fitch parameterization (in `phys/module_wind_fitch.F`) only works in combination with the Mellor-Yamada Nakanishi and Niino Level 2.5 (MYNN2) Planetary Boundary Layer (PBL) scheme, which is itself a parameterization to predict the sub-grid scale turbulence effects in the PBL (Nakanishi and Niino 2009). TKE is not a main prognostic variable in WRF, meaning that it is only active with some of the PBL schemes, including the MYNN2, but not all. In the MYNN2 PBL scheme, the WRF model does not predict TKE evolution three-dimensionally, but rather in each vertical column separately, via a 1-D version of the TKE equation that contains only a dependency on the vertical coordinate z (Nakanishi and Niino 2009; Fitch et al. 2012). In the first implementation of the MYNN2 PBL scheme (WRF v. 3.1 to 3.4), as well as in the default configuration since v. 3.5, there is no horizontal advection of TKE from one column to another because TKE is not passed further to the transport schemes (i.e., horizontal and vertical advection and diffusion). What this means for wind farm wakes is that, in the default setup of the Fitch parameterization, the turbulence in the wake cannot be advected around horizontally in the domain, not because of a fault in the Fitch parameterization itself, but rather because TKE is not advected by default with the MYNN2 PBL scheme. A workaround to this issue was introduced in WRF v. 3.5 via the flag `bl_mynn_tkeadvect`, which can be activated in the `namelist.input` file precisely to allow for TKE to be advected horizontally between grid cells within the MYNN2 PBL scheme. The way this flag works is that the TKE created by sub-grid processes (e.g., a wind farm), which normally would remain in the vertical column and therefore would not be visible to the nearby cells (parallel case) or the rest of the domain (serial case), is stored in a scalar array called `QKE_ADV`, which is visible to the nearby cells (parallel case) and to the entire domain (serial case). With this type of array, there is no need to add advection and horizontal diffusion functions to treat `QKE_ADV` because this is automatically done in the WRF code. By contrast, TKE is not a scalar array in WRF. However, a code bug is present when the flag bl_mynn_tkeadvect is set to true, such that the scalar array QKE_ADV is not properly updated, as described in the next section 3.b.

In the MYNN2 PBL scheme, the relevant variable is QKE, defined as twice the turbulent kinetic energy. We will use therefore QKE in the next section, which deals with the WRF code, but TKE in the rest of the paper, because QKE is not a commonly used variable.

b. Code bug

The flowchart of the relevant processes that affect QKE in the WRF model when the Fitch wind farm parameterization is turned on is shown in Figure 1a (left). Note that the scalar variable QKE_ADV is only active if the flag bl_mynn_tkeadvect is set to true in file namelist.input. If the flag bl_mynn_tkeadvect is set to false or not set at all, which is the default in WRF, then only the variable QKE is active, but it is not advected around in the domain because QKE is not initialized as a global scalar and therefore it is not passed to the WRF dynamic core for advection and horizontal mixing.

Let us first consider the default case, in which bl_mynn_tkeadvect is set to false (i.e., ignore all the flowchart elements that contain QKE_ADV in Figure 1a). In such a case, the QKE at each column, with or without wind turbines, is calculated by the MYNN PBL scheme as a function of only the relevant variables in the column, thus no QKE advection can occur by design anywhere. After the PBL tendencies have been calculated by the MYNN PBL scheme, the updated QKE enters the Fitch parameterization, where additional QKE is added at the grid cell(s) of the wind farm due to the wind farm itself. Note that this QKE never leaves the grid cell(s) of the wind farm and therefore does not affect the rest of the domain. At the next time step, the QKE in the column(s) of the wind farm is spread upward and downward and diffused by the PBL processes, but more QKE is added by the wind farm. The process is repeated over and over and eventually the column(s) of the wind farm is filled with a huge amount of QKE (as shown later), because no advection processes are present to remove it. Other meteorological variables, such as wind speed and temperature, at the grid cell(s) of the wind farm are obviously greatly affected by this huge and unrealistic QKE injection, whereas the rest of the domain is perfectly unaffected by it (Table 1, left column), as we will demonstrate in the Results section.

Let us consider next the case when the flag `bl_mynn_tkeadvect` is set to true. This flag was introduced in WRF V3.5 precisely to solve the issue of the lack of advection of QKE and it is recommended to be set to true if the Fitch wind farm parameterization is to be used. The idea behind it was to have a new global scalar variable, called `QKE_ADV`, which stores QKE after it is updated by the various PBL scheme processes and which is passed to the WRF dynamic core to be advected and mixed around in the domain at all grid cells, not just those with the wind farm. However, due to the bug, QKE at the wind farm cells(s) includes the TKE generated by the wind farm in the Fitch parameterization, but `QKE_ADV` does not because `QKE_ADV` is not updated after the call to the `module_wind_fitch.F` (Figure 1a). Therefore the QKE added by the wind farm, again, never leaves the grid column(s) where the wind farm is, but, contrarily to the previous case, it does not accumulate in time in the grid column(s) of the wind farm because QKE is reset to `QKE_ADV` at beginning of each time step. This means that, at the grid column(s) of the wind farm, the QKE values that are written to the WRF output file at end of each time step are effectively just the QKE calculated by the PBL scheme (affected by the wind shear profile induced by the wind farm) plus QKE added by the wind farm. This also means that the other meteorological variables, like wind speed and temperature near the ground, in the grid cell(s) of the wind farm are not affected by the QKE added by the wind farm itself because, again, `QKE_ADV`, which is the initial value of QKE at the next time step, is never updated with the QKE added by the wind farm. In the rest of the domain, the wind speed deficit in the wake behind the wind farm is properly simulated by the WRF model (aside from a small error caused by the lack of sufficient QKE in the grid cell(s) of the wind farm). Some QKE is also generated downstream in the wake as a result of the increased wind shear above hub height and some is removed due to the reduced wind shear below hub height (Table 1, right column). This new QKE in the wake is also properly advected around, but it is too small overall, as shown later.

The fix to the bug that is present in WRF when the flag `bl_mynn_tkeadvect` is set to true and when the Fitch parameterization is on is to update the variable `QKE_ADV` after the call to `module_wind_fitch.F` within `module_pbl_driver.F`, as shown in Figure 1b. With this easy bug fix, the added QKE by the wind farm at each time step is correctly added to the global scalar `QKE_ADV` and therefore properly advected around in the wake of the wind farm. Also, at the wind farm cells, the PBL tendencies are properly accounting for the effect of QKE induced by the wind farm from the previous time step.

These incorrect QKE results, deduced purely from the flow of the WRF code in Figure 1 and summarized in Table 1, will be proven with ad-hoc simulations in the Results section. We would like to point out that no error is present in the Fitch parameterization per se, but rather in the way it is inserted in the WRF code. The proposed bug fix, i.e., setting `QKE_ADV = QKE` after the call to the Fitch parameterization, is simple and perfectly effective when the flag `bl_mynn_tkeadvect` is set to true. There is no fix for the issues that arise when the flag `bl_mynn_tkeadvect` is set to false (or not set), since they are not exactly a code bug, but rather an inconvenient consequence of neglecting TKE advection by default in the MYNN PBL scheme. It is therefore recommended that, in addition to, of course, adding the bug fix described above, the WRF code be modified in such a way that, if the Fitch parameterization is activated, `bl_mynn_tkeadvect` be automatically set to true.

c. Value of C_{TKE}

The second issue addressed in this paper is the value of the coefficient C_{TKE}, defined in Eq. 2. Remember that C_T and C_P are the thrust and power coefficient, respectively, both of which are a function of hub-height wind speed U_h and are generally provided by the turbine manufacturers. C_T is the fraction of the momentum of the air velocity field that is transferred to the blade velocity field as a consequence of the air pressure drop behind the rotor. C_P is the fraction of the power available in the air flow that becomes electric power, thus it is always lower than C_T because energy is lost to turn the shaft, the generator, and the gears (if present), and due to other electrical losses.

In the Fitch parameterization, the tendency equation for TKE at the grid cell(s) of the wind farm is given by Eq. 3. What Eq. 3 implies is that mechanical and electrical losses in the turbines are zero and that all of the energy left after conversion to electricity generates TKE. Thus, as stated by the authors themselves in Fitch et al. (2012), “the TKE source is overestimated” and C_{TKE} should be refined more accurately “if data regarding the losses in the turbines under study are known”. Other evidence in the literature indicates that this estimate of C_{TKE} is too high. For example, (Abkar and Porté-Agel 2015b, their Figure 5) showed with Large-Eddy Simulation that the added TKE by wind farms (18 to 32 turbines, with different spacings) calculated using Eq. 3 is too high by at least 50% and by up to 230%, depending on the wind farm configuration. Similar conclusions were also reached by (Pan and Archer 2018, their Figure 6), who found overestimates of turbine-generated TKE in a 48-turbine wind farm by up to 220% when the Fitch parameterization was used with the WRF model. Not surprisingly, the resulting TKE profiles over the wind farm also were overestimated by up to 150% (Pan and Archer 2018, their Figure 8).

We propose that the value of C_{TKE} in the Fitch parameterization be reduced to 25% of its original value, as demonstrated in Section 4. We recognize that there is not one value that will work for all farms and all resolutions because the added TKE by a wind farm is a complex physical phenomenon that depends on more than just the thrust and power coefficients. However, the current formulation of the Fitch parameterization, especially after the bug fix proposed in the previous section, would dramatically overestimate the TKE added by the wind farm and therefore even a general correction, like the 25% factor proposed here, will give more realistic results than no correction at all.

We would like to point out that the combination of the under-estimation of TKE in the farm grid cell from the code bug (Table 1) and the over-estimation of TKE in the farm grid cell caused by the excessively-high value of C_{TKE} compensate for each other in such a way that the resulting profile of TKE is somewhat realistic. This is likely the reason why the bug has not been identified before.

3. Methods

a. WRF setup

We used the WRF model version 4.1.2 in idealized simulations with a domain of 40 km $\times$ 40 km $\times$ 10 km in the x, y, and z directions, respectively. The horizontal grid resolution is 1 km and the vertical resolution is 6.3 m near the surface, stretched above to a 225.8-m grid spacing at the domain top, with a total of 51 vertical levels. The turbine selected for the simulations is the NREL 5 MW, with a hub height H = 90 m and a diameter D = 126 m. There are 9 grid levels that intersect the turbine rotor. The flow is driven by a pressure gradient that would give a geostrophic wind of about 9 m/s at hub height from the wind direction 225° (u = 10.5 m s^{-1} and v = 5.4 m s^{-1}). Open boundary conditions are applied at the lateral boundaries. The bottom surface is set as water, with surface roughness calculated in the surface layer scheme (the revised MM5 Monin-Obukhov scheme by Jiménez et al. (2012)). At the top of the domain, a Rayleigh damping layer is applied within the top 1000 m of the domain. The Coriolis parameter is 1.11×10^{-4} s^{-1} at a latitude of 50°N.

For the physical and dynamics options, we turned off the surface flux and radiation schemes. Thus all the simulations are performed under neutral stability conditions. The sf_sfclay_physics is set to 1, which provides a necessary surface momentum drag of the water body (Jiménez et al. 2012). The boundary layer scheme is MYNN 2.5 level TKE scheme (Nakanishi and Niino 2009), which is the only available option working with the Fitch parameterization. The scalar_adv_opt is set to 2 (i.e., monotonic advection), which helps suppress unrealistic oscillations from sharp gradients of TKE near the turbine.

The simulation is run first for 3 days without a wind turbine, to ensure that the pressure gradient, Coriolis force and surface friction force have come into balance. Then another 6 hours are run with the single wind turbine placed at the center of the domain. The instantaneous data after the 6 hours are used. Five test cases are designed:

1. Case 1: the flag `bl_mynn_tkeadvect` is set to false (default configuration);

2. Case 2: the flag `bl_mynn_tkeadvect` is set to true (control case);

3. Case 3: the flag `bl_mynn_tkeadvect` is set to true but the TKE source from the turbine is forced to be zero by imposing $C_{TKE} = 0$. The purpose of this run is to prove that its results at the grid cells without the turbine are the same as those of Case 2, effectively proving that the added TKE from the wind farm is, incorrectly, not affecting the domain, due to the bug;

4. Case 4: the flag `bl_mynn_tkeadvect` is set to true and the bug fix described in section b is implemented to allow for proper TKE advection in the domain.

5. Case 5: as Case 4, but with the proposed reduced value of C_{TKE}.

b. LES setup

The LES results were obtained with the SOftware for Wind Farm Applications (SOWFA), an OpenFOAM-based set of tools, including an actuator line model for the wind turbine blades, that was developed by the National Renewable Energy Laboratory (NREL) to resolve the details of the flow around turbines (Churchfield et al. 2012a,b). SOWFA has been used successfully in many studies to simulate wakes of turbines under a variety of atmospheric stability conditions and grid/time resolutions (Archer et al. 2013; Fleming et al. 2014; Ghaisas and Archer 2016; Martínez-Tossas et al. 2015; Bhaganagar and Debnath 2015; Han et al. 2016; Ghaisas et al. 2017; Chaudhari et al. 2017; Archer and Vasel-Be-Hagh 2019). The domain used here is 3000 m x 3000 m x 1020 m with a single wind turbine in the middle, the same idealized 5 MW NREL turbine used in the WRF simulations with D = 126 m and H = 90 m. The initial resolution is 200 x 200 x 68 grid points in x, y, and z, respectively, corresponding to grid cells of approximately 15 m in all directions. The domain is then further refined to $\sim$7.5 m everywhere, except around the turbine in a volume of size 14D (10D downstream and 4D upstream) x 6D x 400 m, where the resolution is $\sim$3 m (Figure 2). The initial conditions are the same as in WRF (neutral stability up to 700 m, where a 100-m thick inversion layer of 8°C of strength caps the boundary layer) and the flow is forced to maintain an average wind speed of 9 m/s from the 225° wind direction at hub height.

A "precursor" run without the wind turbine and with cyclic lateral boundary conditions is conducted for 12,000 s to reach a quasi-steady turbulent flow, then for an additional 2000 s to save the boundary values. Then, the simulation is restarted at 12,000 s but with the turbine in the domain center (called the "windplant" run) and with the saved boundary conditions from the precursor run. This initialization procedure, which is typical with SOWFA (Churchfield et al. 2012a; Archer et al. 2013), allows for the results to be effectively non-periodic, because the inlet boundary values are unaffected by the turbines themselves, as in the real world. The sub-grid scale turbulence model is the standard One-Equation Eddy Viscosity model in OpenFOAM but with some small modifications, such as buoyancy production (none in this case), specific to atmospheric flows, with the tunable coefficients ce = 0.93 and ck = 0.0673.

To allow for a comparison between the fine-resolution (3–7.5 m) LES results and the coarse-resolution (1000 m) WRF results, the LES results are plane-averaged over all the grid points in selected 1000 m x 1000 m squares, numbered from 0 to 2 in Figure (Figure 2). Square 1 is used to compare against WRF results obtained at the grid cell of the wind turbine, Square 2 for the next grid cell downwind, and Square 0 for undisturbed conditions. All squares contain refined and non-refined cells. Turbine-generated TKE and wind speed deficits are calculated as the difference between the value in the square of interest – 1 or 2 – and that in Square 0, treated effectively as the control. A more natural choice for the control would have been the lower-left square in the domain. However, the lower-left square was not selected because the refinement zone introduces some numerical noise in it and because it is too affected by the two inlet boundaries. Square 0 was selected because it is sufficiently far from the inlet boundaries to have developed a fully turbulent flow, it is partially in the refinement zone, and yet it is not affected by the turbine wake. Square 3 was used for comparison with coarser resolution runs in section d.

4. Results

The discussion in this section focuses on the WRF results obtained after four hours of simulation time, after which a steady state was reached such that the results did not change significantly any more.

a. Horizontal cross-sections

As expected from Table 1, when the flag `bl_mynn_tkeadvect` is false (Case 1), there is no wake to speak of, as the only grid point with TKE greater than the background value of approximately 0.79 $m^2\ s^{-2}$ is that of the wind turbine in the middle of the domain (Figure 3a). Figure 3a-e is zoomed over the center of the domain and is designed to show the exact TKE values at the individual grid cells. The value at the grid cell of the turbine is very high, exceeding 1.9 $m^2\ s^{-2}$ at hub height, while the LES results at most reach 2.5 $m^2\ s^{-2}$ but only in the most turbulent portions of the wake (Figure 3f). A region with slightly reduced wind speed (8.9 $m\ s^{-1}$ compared to 9.0 $m\ s^{-1}$ in the surrounding air, thus about 2% lower) is visible in the wind speed field (Figure 4a), extending over 10 km downwind of the turbine. Because the wind speed difference is so small, it cannot even be considered a wake.

However, even when the flag `bl_mynn_tkeadvect` is true (Case 2), there is still no sign of a wake in the TKE distribution (Figure 3b) because of the bug. Only the grid point of the wind turbine in the center has a value of TKE that is slightly higher than the background, 0.87 $m^2\ s^{-2}$, which corresponds to the amount of TKE added by the turbine just in the last time step and which does not affect the rest of the domain. Because the added TKE at the grid cell is lower than in Case 1, there is less turbulence to replenish the wind speed deficit. The wind speed deficit in the wake, therefore, is strong enough to cause an actual weak wake, extending to approximately 7 km downwind (dark blue shade in Figure 4b), with a wind speed about 4% lower than that of the surrounding air. As a result of the two compensating errors – too low added TKE and too high C_{TKE} – the TKE value at the grid cell of the turbine is actually very close to the LES value ($\sim$0.9 $m^2\ s^{-2}$, obtained by adding the WRF background value of approximately 0.79 $m^2\ s^{-2}$ to the turbine-generated TKE at hub height, approximately 0.11 m^2 s^{-2} from Figure 6c). Probably, this is why the bug was not identified before.

To demonstrate the effect of the code bug, namely that the added TKE at the grid cell of the turbine does not affect the rest of the domain, Figure 3c shows the TKE distribution when C_{TKE} is actually set to zero intentionally (Case 3), to prevent any turbulence caused by the turbine from being added to the atmosphere. Aside from the grid cell of the wind turbine, the TKE distribution in the rest of the domain is perfectly identical in Cases 2 and 3. Similarly, the wind speed distribution in the wake and in the rest of the domain is exactly identical in Cases 2 and 3 (Figure 4b,c). Again, setting the flag `bl_mynn_tkeadvect` to true does not allow for any actual advection of the TKE added by the turbine in the rest of the domain because of the code bug.

When the code bug is fixed, but C_{TKE} is equal to its default value (Case 4), a turbulent wake is finally formed downwind of the turbine, notable from both the reduced wind speed (Figure 4d) and the higher TKE (0.80-1.00 m^2 s^{-2}) than the background (Figure 3d). However, the value of TKE at the grid cell of the wind turbine, 1.35 m^2 s^{-2}, is over-estimated (LES indicate $\sim$0.9 m^2 s^{-2}, as explained earlier) due to the excessive value of C_{TKE}. The wind speed deficit in the wake is less strong than in Cases 2-3 and the wake is rather short, because of the excessive TKE at the grid cell of the turbine causing excessive mixing and replenishing the wind speed field too quickly (Figure 4b-d).

Finally, Figures 3e and 4e show the results when both the code bug and the C_{TKE} issue are solved. The TKE at the grid cell of the wind turbine in the center is 0.94 m^2 s^{-2}, very close to the LES (Figure 3f), and it is correctly advected downwind, where it adds to the TKE generated by the shear caused by the wind speed deficit. Note that the resulting distribution of the wind speed deficit in the wake is similar to that in Cases 2 and 3 (Figures 4b-c) because of the compensating errors.

b. Vertical cross-sections

We analyze next the vertical distribution of TKE in cross-sections aligned with the wind direction, i.e., 225° (Figure 5).

In Case 1, the TKE added by the wind turbine at each step keeps adding on into the grid cells of the wind turbine exclusively, since there is no horizontal TKE advection in the MYNN scheme when the flag `bl_mynn_tkeadvect` is not set. As a result, TKE has nowhere to go except vertically, thus it fills the entire column above and below the wind turbine (Figure 5a), which is completely unrealistic (Figure 5f). Case 1 was the only case that did not actually reach a steady state after 4 hours, as the added TKE continued to grow with time in the column of the wind turbine. If the flag `bl_mynn_tkeadvect` is not set to true, the results at the wind turbine cell are unrealistic.

Cases 2 and 3 are, again, identical except for the grid cells directly intersected by the wind turbine rotor (Figures 5b,c). This proves once again that, even though TKE should be advected around and affect the rest of the domain, it effectively does not, due to the code bug. Whereas in Case 1 the column of the wind turbine responds to the added TKE (Figures 5a), the code bug acts in such a way that there is basically no effect of the added TKE, not even in the column of the wind turbine (Figures 5b,c). Note that there is a slight reduction in TKE below hub height downwind of the turbine in both cases, as suggested by Archer et al. (2019), a result of the reduced wind shear below the rotor that causes a decrease in TKE production.

In Case 4, a wake is finally present downwind of the turbine in the TKE field (Figure 5d), extending approximately 4 km at hub height. Advection and local shear-generation both contribute to the TKE in the wake, but, due to the excessive value of C_{TKE}, the turbulence of the wake reaches unrealistically high values near the ground right below the turbine (compare against LES results near the ground in Figure 5f and 6c).

Case 5 is able to produce a realistic wake, with TKE of the order of 0.9 $m^2 s^{-2}$ at the grid cell of the turbine, reaching approximately 3 km downwind (at hub height) and not touching the ground.

c. Vertical profiles

The two issues described in this paper, the code bug and the excessive value of C_{TKE}, have not been identified before because their combined effect is extremely difficult to detect, since it causes the simulated vertical TKE profile at the wind turbine grid cells to be rather close to the observed or LES-simulated one when TKE advection is activated. In other words, the TKE profile is correct but for the wrong reasons (plus the rest of the domain is incorrectly unaffected by the added turbulence). This can be appreciated in Figure 6c, where the profile of turbine-generated TKE for Case 5 (the recommended configuration) is very similar to the LES profile at the grid cell of the wind turbines. Turbine-generated TKE is defined as the difference between the TKE in the various Cases and that in the run without the turbine. Case 1, as already discussed, injects too much TKE over the grid cells of the wind turbine and Case 4, despite the bug fix, also injects too much TKE because of the excessive value of C_{TKE} (Figure 6a). Case 5 is correct above the wind turbine (Figure 6c) and is the closest to the LES in the downstream wake (Figure 6d), except for Case 4 which, paradoxically, exhibits a good match with the LES results but for the wrong reasons.

Below the rotor, the LES results indicate that turbine-generated TKE is reduced both at the grid cell of the turbine and in the one downwind (Figure 6c-d), as discussed in Archer et al. (2019). The WRF simulations do not reproduce this behaviour due to the low vertical resolution. However, a lack of TKE enhancement is shown in the grid cells immediately downwind of the wind turbine in all cases except Case 4.

Cases 2 and 3 are identical downstream, but are slightly different in the wind turbine cells, because Case 3 truly injects no TKE at all, but Case 2 injects a small amount of TKE, just the TKE that was generated by the wind turbine in the last time step. Case 1 shows lower TKE than all other cases downwind of the wind turbine (Figure 6b), as expected because not even the TKE generated by the increased shear in the upper part of the wake is advected around in Case 1.

Note that no simulation with the WRF model can reproduce the secondary TKE maximum shown in the LES results (Figure 3f and 6d), which is caused by the combination of the further development of turbulence structures induced by the wind turbines and the strong wind shear in the upper part of the wake. These subgrid-scale turbulence structures cannot be parameterized by simply adding a TKE source term in the PBL scheme in WRF. In addition, the wind shear in the wake ends up being diffused in the entire grid cell that contains the wake and therefore, at the resolved scale, it is not sufficient to generate TKE.

The wind speed deficits are generally underestimated in WRF for all cases (Figure 7). At the cells intersected by the wind turbine rotor, the profiles from all cases are close to each other and lower than the LES results by up to 50% (Figure 7a). Below the rotor, however, Cases 1 and 4, which are the cases that injected the most TKE, show an acceleration of the flow near the ground that causes a negative deficit. This “jet” is not present in the LES results. Cases 2, 3, and 5, in fact, do not produce any such feature. This suggests that this jet, which was actually simulated in the literature for a single wind turbine (Xie and Archer 2015) and possibly observed in the wake of a wind farm (Rajewski et al. 2013), is more likely to form in the presence of high TKE in the wake.

Downwind of the turbine, again, the slow speed near the ground from the LES is not well represented in Cases 1 and 4, which still show a jet, but it is best simulated in Case 5. All cases do a reasonably good job at reproducing the wind speed deficit in the rotor region.

d. Sensitivity to grid resolution

It is likely that the optimal correction factor to the C_{TKE} coefficient depend on a variety of factors, from grid resolution to wind farm layout to atmospheric stability. The proposed correction factor, 0.25, is the best for the case presented here, but it may or may not be for other cases. A full analysis of this issue is beyond the purposes of this paper, mainly because any validation would require additional computationally-intensive LES runs, possibly over larger domains.

Here, without running additional LES, we are able to assess the sensitivity of the correction factor to a decrease of the WRF grid resolution by a factor of two, i.e., 2 km x 2 km. We focused on Cases 4 and 5, with various values of the correction factor (0.1, 0.25, and 0.5). Vertical profiles of turbine-generated TKE at lower resolution (Figure 8a) show the same pattern as those at high resolution (Figure 6), with unrealistically high values for Case 4 and substantial improvements in Case 5. The best match over the rotor region was reached with a correction factor of 0.25, although a value of 0.5 gives the best match above the rotor. For the wind speed deficit, the profiles are basically the same regardless of the value of C_{TKE} (Figure 8b). The LES results were averaged over a square of 2 km x 2 km centered at the turbine location in the middle of the domain, identified as Square 3 in Figure 2.

In conclusion, a correction factor of 0.25 for C_{TKE} appears to be a robust first estimate for the horizontal grid resolutions considered here, i.e., 1 km and 2 km.

5. Conclusions

In summary, regardless of the flag `bl_mynn_tkeadvect`, TKE advection is improperly treated in the WRF model in the presence of a wind farm modeled with the Fitch parameterization. As a consequence, all the other meteorological variables, both at the wind farm cells and in the rest of the domain, are incorrectly predicted. When the flag is off, TKE is greatly overestimated at the wind farm cells, temperature and other meteorological variables at the wind farm cells are affected by this excessive TKE, while the rest of the domain is not affected at all by the farm in any way. When the flag is turned on, TKE is greatly underestimated at the wind farm cells, temperature and other meteorological variables at the wind farm cells are not affected at all by this TKE, and the rest of the domain is affected by only the TKE formed in the wake by the altered wind shear in the wake.

A code bug and the incorrect neglect of electro-mechanical losses are the reasons for the incorrect treatment of TKE in the WRF model with the Fitch parameterization. These two issues interacted in a subtle way with one another, causing compensating errors that generated somewhat realistic TKE and wind speed deficit profiles. This is probably why these issues were not noticed before.

Here we proposed a simple code change that will fix the code bug and will allow for proper advection of the TKE generated by the wind farm, in addition to that generated by shear in the wake. We also proposed a preliminary correction of the value of the C_{TKE} coefficient to one quarter of its original value, which gives us the best match to LES results for a single turbine positioned in the grid cell center and is dramatically better than keeping the original value, for both 1 km and 2 km horizontal grid resolutions. In order to provide better estimates of the C_{TKE} coefficient for other configurations, future work should investigate its dependency on wind turbine position in the grid, farm size (i.e., number of wind turbines), grid resolution, atmospheric stability, array layout, wind direction, among other properties.

The main limitation after the fixes is that turbine-generated TKE is still not large enough in the wake downstream of the grid cell with the turbine. The exact impact on the resolved variables is unknown, but it expected to be non-negligible. It is our hope that this study will provide the stimulus for authors of past studies to fix the code bug and possibly rerun their simulations to confirm or revise the validity of their findings. We reported the bug and correction factor for C_{TKE} to the github repository for WRF (`https://github.com/wrf-model/WRF/pull/1235`).

Acknowledgments. The issues discussed in this paper were discovered and resolved during projects n. 0040420490, sponsored by the U.S. Bureau of Ocean Energy Management, and n. 1564565, sponsored by the U.S. National Science Foundation's Division of Atmospheric and Geospace Sciences. The research was conducted on the Caviness high-performance computer clusters of the University of Delaware.

References

Abkar, M., and F. Porté-Agel, 2015a: A new wind-farm parameterization for large-scale atmospheric models. *Journal of Renewable and Sustainable Energy*, **7 (1)**, 013 121, doi:doi:10.1063/1.4907600.

Abkar, M., and F. Porté-Agel, 2015b: A new wind-farm parameterization for large-scale atmospheric models. *J Renew Sust Energy*, **7 (1)**, 013 121.

Adams, A. S., and D. W. Keith, 2013: Are global wind power resource estimates overstated? *Environ Res Lett*, **8 (1)**, 015 021.

Archer, C. L., S. Mirzaeisefat, and S. Lee, 2013: Quantifying the sensitivity of wind farm performance to array layout options using large-eddy simulation. *Geophys Res Lett*, **40 (18)**, 4963–4970.

Archer, C. L., and A. Vasel-Be-Hagh, 2019: Wake steering via yaw control in multi-turbine wind farms: Recommendations based on large-eddy simulation. *Sustainable Energy Technologies and Assessments*, doi:10.1016/j.seta.2019.03.002.

Archer, C. L., S. Wu, A. Vasel-Be-Hagh, J. F. Brodie, R. Delgado, A. St. Pé, S. Oncley, and S. Semmer, 2019: The VERTEX field campaign: Observations of near-ground effects of wind turbine wakes. *Journal of Turbulence*, **20**, 64–92, doi:10.1080/14685248.2019.1572161.

Baidya Roy, S., S. Pacala, and R. Walko, 2004: Can large wind farms affect local meteorology? *J. Geophys. Res. Atmos.*, **109 (D19)**.

Barrie, D. B., and D. B. Kirk-Davidoff, 2010: Weather response to a large wind turbine array. *Atmospheric Chemistry and Physics*, **10**, 769–775.

Bhaganagar, K., and M. Debnath, 2015: The effects of mean atmospheric forcings of the stable atmospheric boundary layer on wind turbine wake. *Journal of Renewable and Sustainable Energy*, doi:10.1063/1.4907687.

Blahak, U., B. Goretzki, and J. Meis, 2010: A simple parameterization of drag forces induced by large wind farms for numerical weather prediction models. *Proceedings of the European Wind Energy Conference & Exhibition*.

Chaudhari, A., O. Agafonova, A. Hellsten, and J. Sorvari, 2017: Numerical study of the impact of atmospheric stratification on a wind-turbine performance. *Journal of Physics: Conference Series*, **854**, 012 007, doi:10.1088/1742-6596/854/1/012007.

Churchfield, . J., S. Lee, J. Michalakes, and P. J. Moriarty, 2012a: A numerical study of the effects of atmospheric and wake turbulence on wind turbine dynamics. *J Turbul*, **13 (14)**, 1–32.

Churchfield, ., S. Lee, P. Moriarty, L. Martinez, S. Leonardi, G. Vijayakumar, and J. Brasseur, 2012b: A large-eddy simulations of wind-plant aerodynamics. *50th AIAA Aerospace Sciences Meeting*, 537.

Fitch, A. C., J. B. Olson, and J. K. Lundquist, 2013: Parameterization of wind farms in climate models. *Journal of Climate*, **26 (17)**, 6439–6458.

Fitch, A. C., J. B. Olson, J. K. Lundquist, J. Dudhia, A. K. Gupta, J. Michalakes, and I. Barstad, 2012: Local and mesoscale impacts of wind farms as parameterized in a mesoscale NWP model. *Monthly Weather Review*, **140 (9)**, 3017–3038, doi:10.1175/MWR-D-11-00352.1.

Fleming, P. A., and Coauthors, 2014: Evaluating techniques for redirecting turbine wakes using SOWFA. *Renewable Energy*, **70**, 211–218, doi:10.1016/j.renene.2014.02.015.

Ghaisas, N., C. Archer, S. Xie, S. Wu, and E. Maguire, 2017: Evaluation of layout and atmospheric stability effects in wind farms using large-eddy simulation. *Wind Energy*, **20 (7)**, doi:10.1002/we.2091.

Ghaisas, N. S., and C. L. Archer, 2016: Geometry-based models for studying the effects of wind farm layout. *J Atmos Ocean Technol*, **33 (3)**, 481–501, doi:10.1175/JTECH-D-14-00199.1.

Han, Y., M. Stoellinger, and J. Naughton, 2016: Large eddy simulation for atmospheric boundary layer flow over flat and complex terrains. *Journal of Physics: Conference Series*, **753 (3)**, doi:10.1088/1742-6596/753/3/032044.

Jacobson, M. Z., and C. L. Archer, 2012: Saturation wind power potential and its implications for wind energy. *Proc Natl Acad Sci*, **109 (39)**, 15 679–15 684.

Jiménez, P. A., J. Dudhia, J. F. González-Rouco, J. Navarro, J. P. Montávez, and E. García-Bustamante, 2012: A revised scheme for the WRF surface layer formulation. *Monthly Weather Review*, **140 (3)**, 898–918, doi:10.1175/MWR-D-11-00056.1.

Keith, D. W., J. F. DeCarolis, D. C. Denkenberger, D. H. Lenschow, S. L. Malyshev, S. Pacala, and P. J. Rasch, 2004: The influence of large-scale wind power on global climate. *Proceedings of the National Academy of Sciences*, **101 (46)**, 16 115–16 120, doi:10.1073/pnas.0406930101, arXiv:1011.1669v3.

Kirk-Davidoff, D. B., and D. W. Keith, 2008: On the climate impact of surface roughness anomalies. *J Atmos Sci*, **65 (7)**, 2215–2234.

Martínez-Tossas, L. A., M. J. Churchfield, and C. Meneveau, 2015: Large Eddy Simulation of wind turbine wakes: Detailed comparisons of two codes focusing on effects of numerics and subgrid modeling. *Journal of Physics: Conference Series*, **625 (1)**, 1–10, doi:10.1088/1742-6596/625/1/012024.

Marvel, K., B. Kravitz, and K. Caldeira, 2013: Geophysical limits to global wind power. *Nat Clim Change*, **3**, 118–121.

Miller, L. M., F. Gans, and A. Kleidon, 2011: Estimating maximum global land surface wind power extractability and associated climatic consequences. *Earth Syst. Dynam*, **2 (1)**, 1–12.

Nakanishi, M., and H. Niino, 2009: Development of an improved turbulence closure model for the atmospheric boundary layer. *J Meteorol. Soc. Japan*, **87 (5)**, 895–912.

Pan, Y., and C. L. Archer, 2018: A hybrid wind-farm parametrization for mesoscale and climate models. *Boundary-Layer Meteorology*, **168 (3)**, 469–495, doi:10.1007/s10546-018-0351-9.

Rajewski, D. A., and Coauthors, 2013: Crop wind energy experiment (CWEX): Observations of surface-layer, boundary layer, and mesoscale interactions with a wind farm. *Bull. Am. Meteorol. Soc.*, **94 (5)**, 655–672.

Volker, P., J. Badger, A. N. Hahmann, and S. Ott, 2015: The explicit wake parametrisation v1.0: A wind farm parametrisation in the mesoscale model WRF. *Geosci Model Dev*, **8 (11)**, 3715–3731.

Vollmer, L., G. Steinfeld, D. Heinemann, and M. Kühn, 2016: Estimating the wake deflection downstream of a wind turbine in different atmospheric stabilities: an LES study. *Wind Energy Science*, **1 (2)**, 129–141.

Wang, C., and R. G. Prinn, 2010: Potential climatic impacts and reliability of very large-scale wind farms. *Atmos Chem Phys*, **10 (4)**, 2053–2061.

Xie, S., and C. Archer, 2015: Self-similarity and turbulence characteristics of wind turbine wakes via large-eddy simulation. *Wind Energy*, **18 (10)**, 1815–1838.

LIST OF TABLES

TABLE 1. Summary of the effects of the incorrect treatment of TKE advection in the WRF model when used with the Fitch wind farm parameterization. The flag `bl_mynn_tkeadvect` is set in the `namelist.inp` file.

	bl_mynn_tkeadvect	
	False	True
QKE at the wind farm cell(s)	Over-estimated	Under-estimated
Met-variables at the wind farm cell(s)	Overly affected	Unaffected
QKE in the rest of the domain	Unaffected	No QKE from wind farm, only QKE shear-generated in wake
Met-variables in the rest of the domain	Unaffected	Affected by no QKE from wind farm, only QKE shear-generated in wake

LIST OF FIGURES

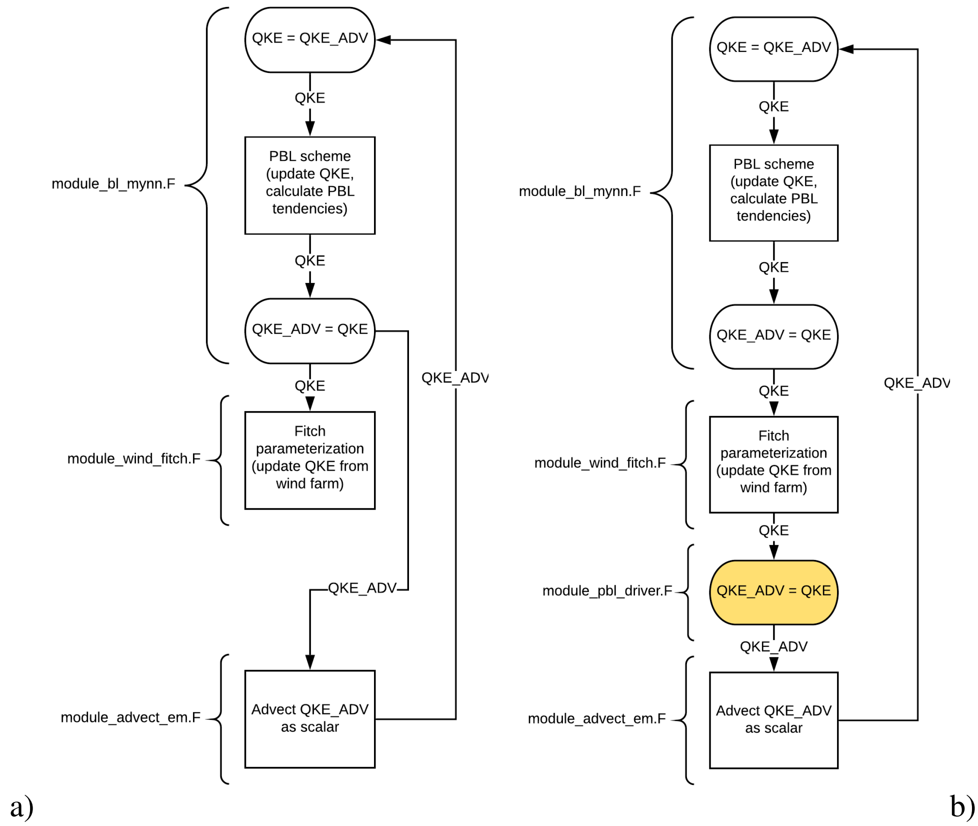

FIG. 1. Flowchart of the treatment of QKE (twice the turbulent kinetic energy) in the WRF model: a) with the bug and b) with the proposed bug fix. Note that the scalar variable `QKE_ADV` is only active if the flag `bl_mynn_tkeadvect` is set to true in file `namelist.inp`.

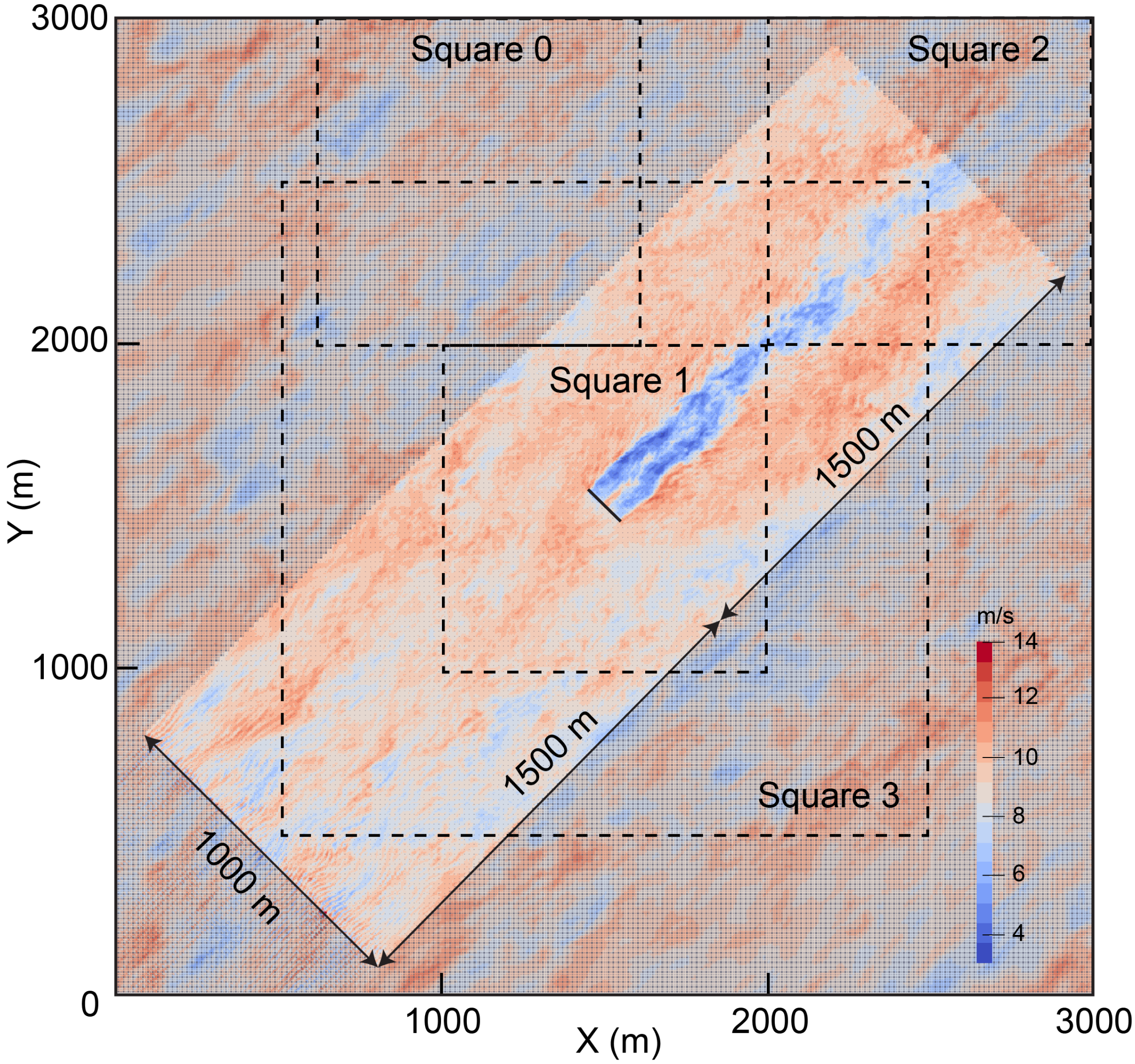

FIG. 2. Horizontal cross-section at hub height (90 m) of instantaneous wind speed (m/s) after 14000 s of the LES simulation. The wireframe of the 3000 m x 3000 m domain is visible and the refinement zone (3000 m x 1000 m) is shown in more vibrant shades. The wind turbine is located in the middle of the domain. Square 1 is used to calculate area-averages to compare against WRF's results at the grid cell of the wind turbines; Square 2 for one grid cell downwind; Square 0 for undisturbed conditions; and Square 3 for comparison against WRF results at coarser resolution (2 km x 2 km).

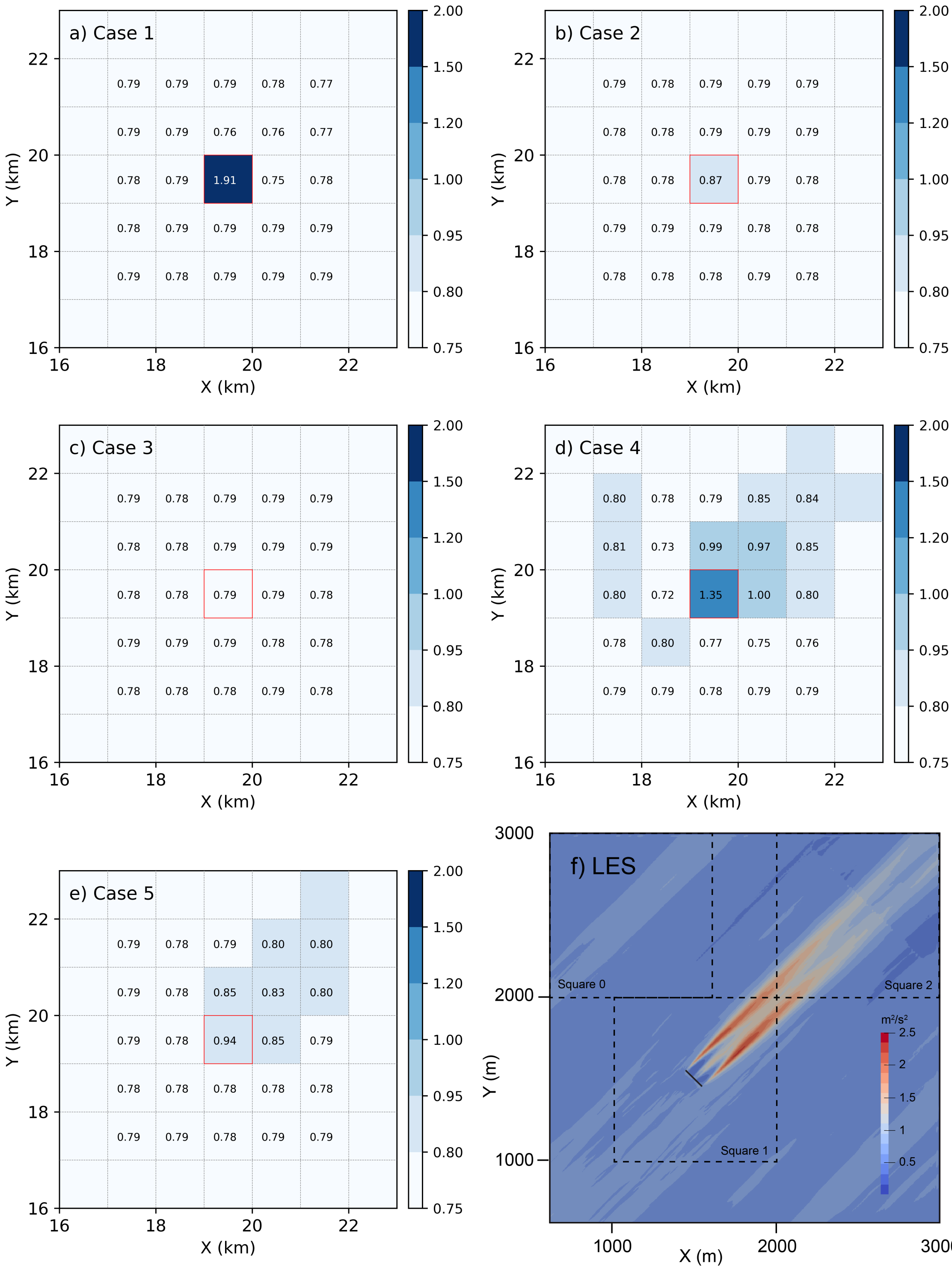

FIG. 3. Horizontal cross-sections of simulated TKE ($m^2\ s^{-2}$) at hub height (90 m) with the wind turbine in the center: a) Case 1 (`bl_mynn_tkeadvect` = false); b) Case 2 (`bl_mynn_tkeadvect` = true); c) Case 3 (`bl_mynn_tkeadvect` = true and C_{TKE} = 0); d) Case 4 (`bl_mynn_tkeadvect` = true and bug fixed); e) Case 5 (like Case 4 but with C_{TKE} reduced to 25%); and f) LES results (note the different axes).

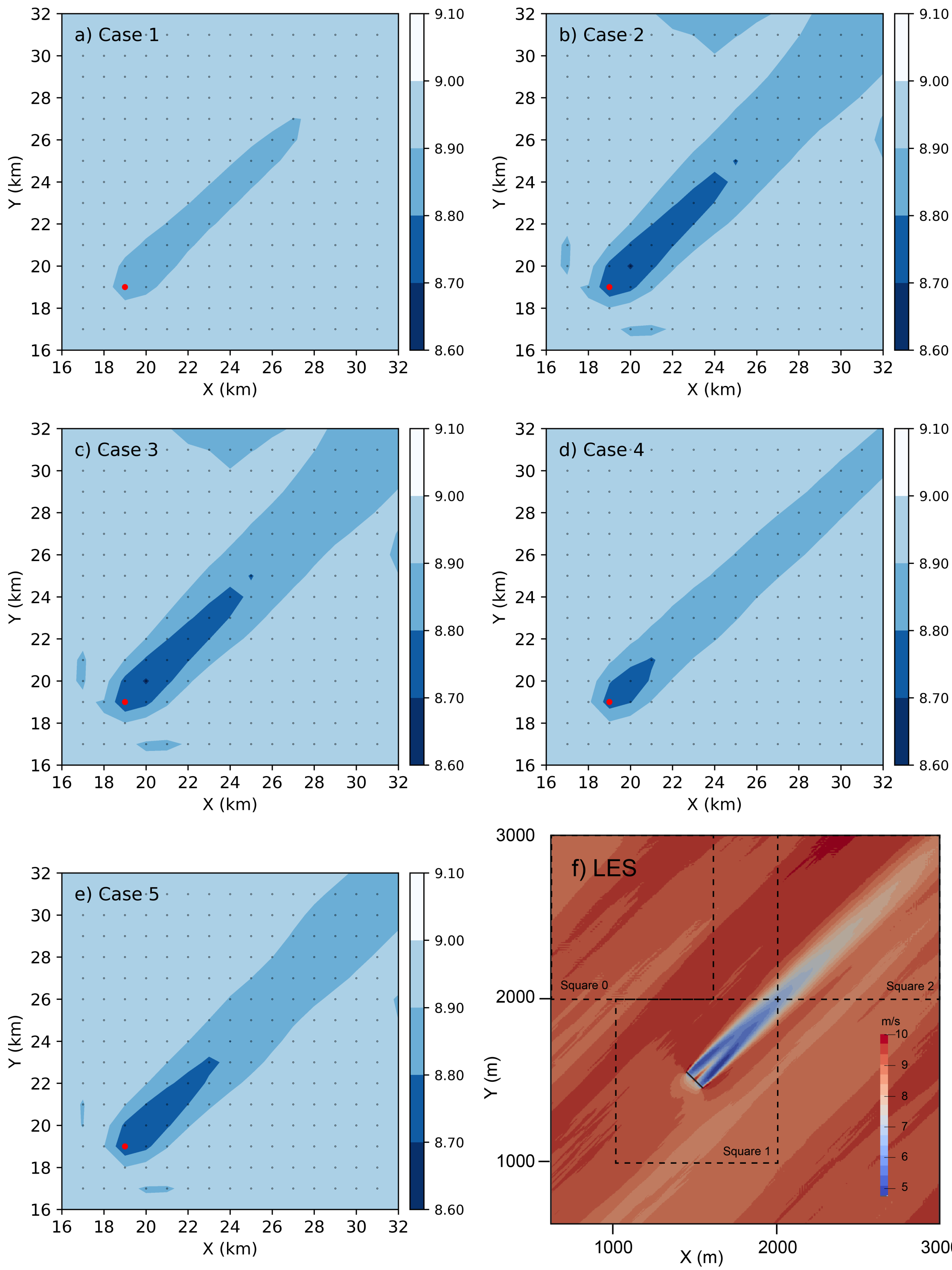

FIG. 4. As in Figure 3 but for wind speed (m s^{-1}) at hub height (90 m).

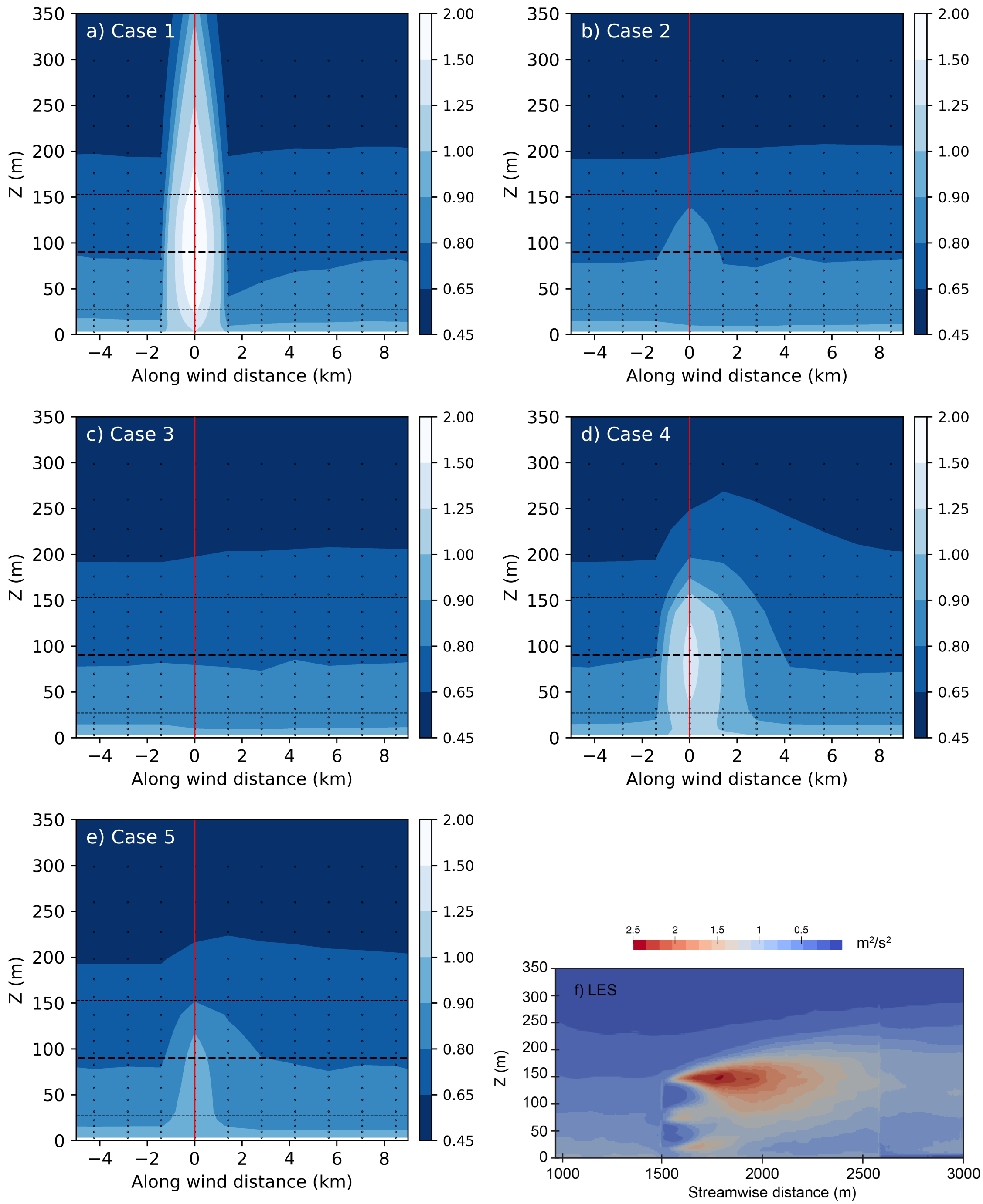

FIG. 5. As in Figure 3 but for vertical cross-sections of simulated TKE ($m^2\ s^{-2}$) along the wind direction 225°.

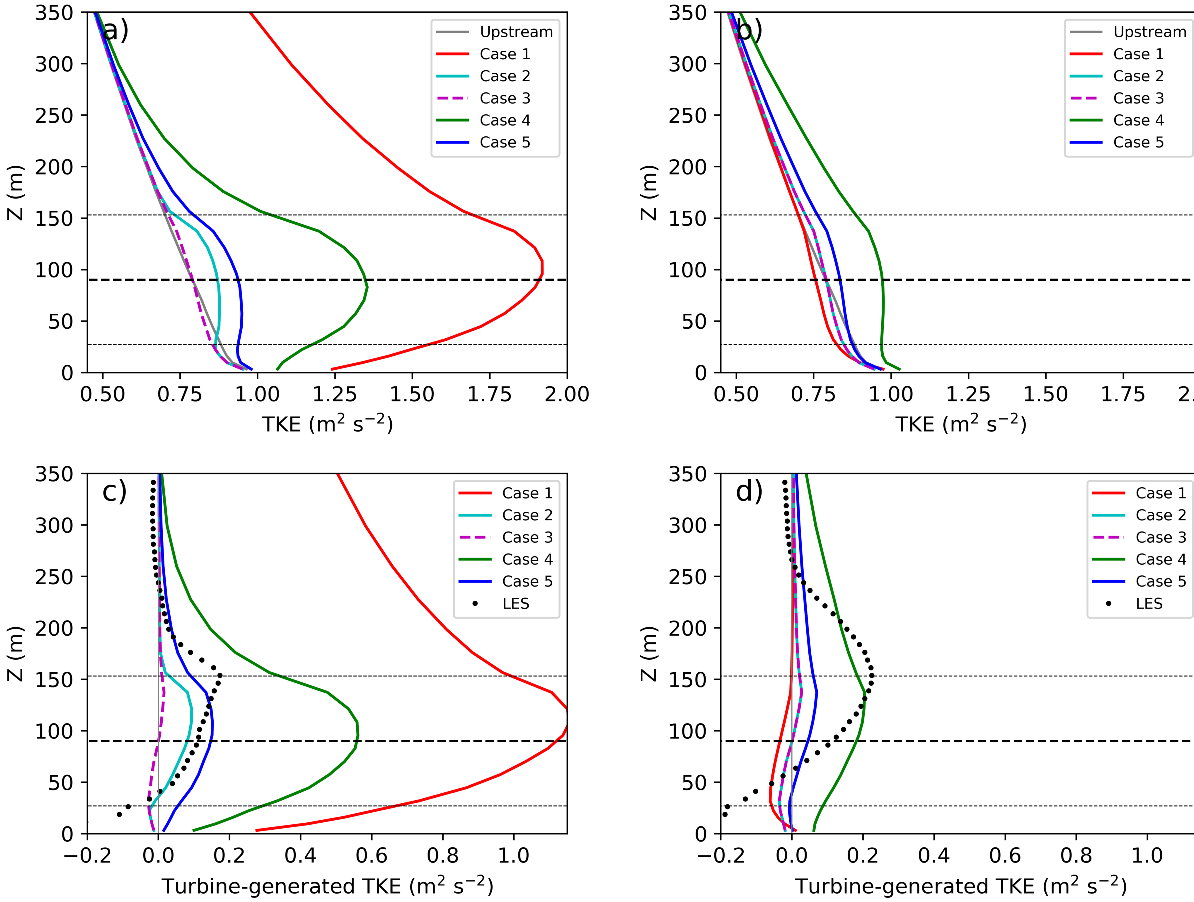

FIG. 6. Vertical profiles from the five WRF cases and the LES run of: a) TKE (m^2 s^{-2}) at the grid cell of the wind turbine; b) TKE one grid cell downwind; c) turbine-generated TKE at the grid cell of the wind turbine (LES: average over Square 1 - average over Square 0, Figure 3f); and d) turbine-generated TKE one grid cell downwind (LES: average over Square 2 - average over Square 0, Figure 3f).

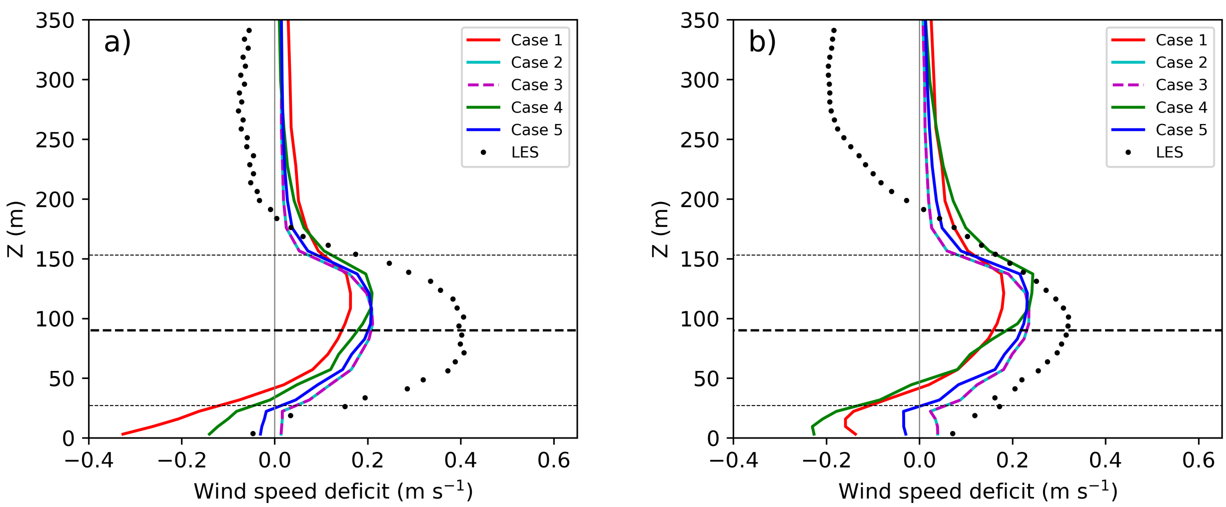

612 FIG. 7. Vertical profiles of wind speed deficit (m s^{-1}) from the five WRF cases and the LES run at: a) the grid cell of the wind turbine (LES: average over Square 0 - average over Square 1, Figure 4f), and b) one grid cell downwind (LES: average over Square 0 - average over Square 2, Figure 4f).

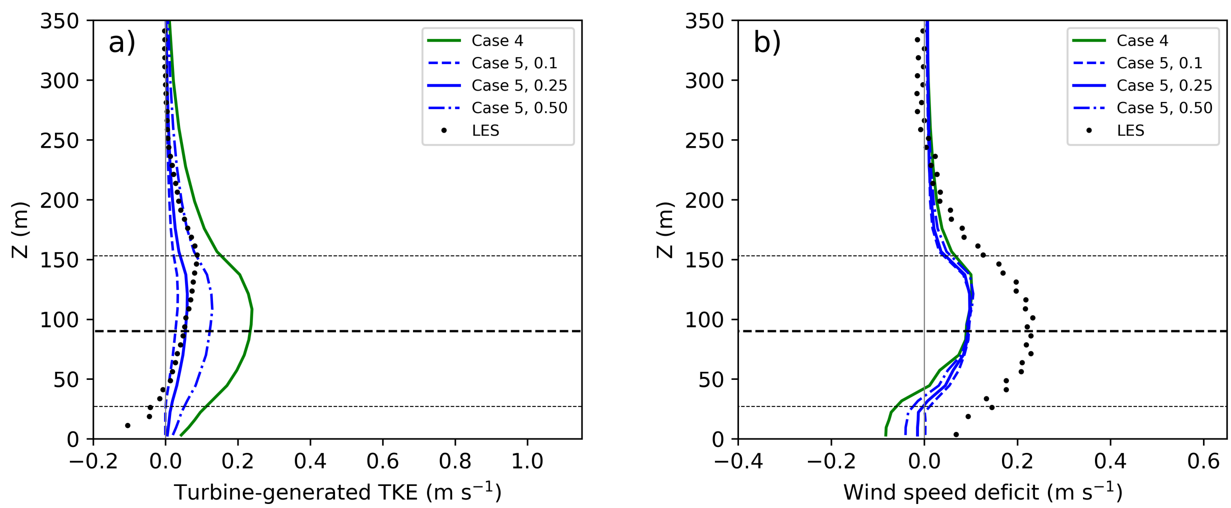

FIG. 8. Vertical profiles of: a) turbine-generated TKE (m^2 s^{-2}) and b) wind speed deficit (m s^{-1}) from Cases 4 and 5 (with various values of the correction factor for C_{TKE}) at the grid cell of the wind turbine from WRF simulations at a grid resolution of 2 km x 2 km. The LES values were obtained as the average over Square 3 - average over Square 0 in a) and as the average over Square 0 - average over Square 3 in b).